

Characterization of Aerosol Delivery for Preterm Infants

JOSE MANUEL LOPEZ-GUEDE¹, IÑIGO ARAMENDIA², UNAI FERNANDEZ-GAMIZ², JAVIER SANCHO², MIGUEL ANGEL GOMEZ SOLAETXE³, ALBERTO LOPEZ-ARRAIZA³, FRANCISCO JOSE BASTERRETXE⁴

¹Systems Engineering and Automatics Department

²Nuclear Engineering and Fluid Mechanics Department

³Department of Nautical Science and Marine Systems

⁴Department of Physical Chemistry

University of the Basque Country (UPV/EHU)

Nieves Cano 12, 01006, Vitoria-Gasteiz, Araba

SPAIN

jm.lopez@ehu.eus

Abstract: - Respiratory Distress Syndrome (RDS) of the newborn is the leading cause of death in premature infants. The current surfactant replacement therapy presents some drawbacks, as it requires the intubation of the newborn and the application of mechanical ventilation, which may induce lung injuries and/or chronic diseases. The upsurge use of non-invasive ventilation techniques in preterm babies, as CPAP, has led to the study of new minimally invasive surfactant therapies. In this paper an inhalation catheter (IC) (AeroProbe, Trudell Medical International), with one central lumen to deliver the liquid and six peripheral lumens to deliver the compressed air, has been tested to study the aerosol generated both experimentally and numerically. An Aerodynamic Particle Sizer (APS 3321, TSI Incorporated) has been used, which provides high-resolution, real-time aerodynamic measurements of particles from 0.5 to 20 μm . Additionally, Computational Fluid Dynamics (CFD) techniques have been used in order to develop a mathematical model to characterize the aerosol generated by the IC.

Key-Words: - Respiratory Distress Syndrome, Aerodynamic Particle Sizer, Inhalation catheter, aerosol.

1 Introduction

Extremely and very preterm infants present cerebral and pulmonary issues due to the immaturity of the lungs, primarily caused by the lack of surfactant. This leads to the Respiratory Distress Syndrome (RDS) of the newborn, which is the leading cause of death in premature babies [1]. This natural substance covers the alveoli, being its main goal to reduce the surface tension and, therefore, to prevent alveolar collapse at the end of the exhalation, retaining enough air to start the next breath. The surfactant replacement therapy implies some drawbacks, as the requirement of intubation and the application of ventilator support techniques, which can result in lung injury and chronic lung diseases (CLD) [2, 3]. In this regard, the neonatologists are focused on new minimally invasive surfactant therapies (MIST) as an alternative to solve the current dilemma; how to deliver exogenous surfactant without invasive techniques when the application of continuous positive airway pressure (CPAP) is not enough. The guidelines recommend nowadays the use of natural surfactants instead of synthetic ones and as early as possible in the course

of RDS [4]. It is also reported a survival advantage with higher initial doses of natural surfactant (200 mg/kg better than 100 mg/kg using poractant alfa) and fewer requirement of a second dose [5].

One alternative therapy is the INSURE technique (Intubation, Surfactant, Extubation) firstly reported by Verder et al. [6] in 1994. It consists in intubating the preterm infant for surfactant administration with quick (within 10 minutes) extubation to nCPAP. Sandri et al. [7] published a randomized controlled trial to evaluate the efficacy of combining prophylactic surfactant and early selective surfactant, with nCPAP in preterm infants. Their results showed that prophylactic surfactant given within 30 minutes of birth was not superior to early selective surfactant in terms of requirement of MV in the first 5 days of life. The tracheal catheterization is the most extensively method studied so far. Dargaville et al. [8] developed the Hobart method, where Curosurf surfactant at a dose of 100 mg/kg is administered using a semi-rigid vascular catheter briefly passed into the trachea beyond the vocal cords. The results showed that

surfactant can be effectively delivered by this technique with a considerably reduction of intubation and MV in the first 72 hours [9]. Currently, they are working on a randomized control trial (the OPTIMIST-A trial) evaluating a total of 606 infants which is expected to be completed in 2020 [10].

The administration of nebulized surfactant is a promising technique to treat lung diseases and especially RDS even though there are still technical issues and challenges to lead. Four clinical trials have been published [11-14] showing that is a feasible and safe technique, however, only one of them [12] has demonstrated good results. Currently, Pillow and Minocchieri are working on a new clinical trial, the CureNeb study, where preterm infants receive either CPAP or CPAP and nebulized surfactant in the first 4 hours of life [15]. Another alternative is the use of perfluorocarbons (PFC) instead of surfactant. Burkhardt et al. [16] have demonstrated that is useful to improve surfactant distribution and that resulted in an improved oxygenation.

One of the main reasons of the low efficiency of nebulized surfactants in these clinical trials is the relative low lung deposition rates (less than 1% of the mass nebulized) with conventional jet and ultrasonic nebulizers [17, 18]. Nevertheless, Goikoetxea et al. [19, 20] have studied the potential to deliver relatively large amounts of surfactants and perfluorocarbons beyond the third generation of branching in a neonatal airway model through an intracorporeal inhalation catheter (IC). Syedain et al. [21] have introduced recently a novel device of narrow gauge (outside diameter < 1mm) to be inserted into an endotracheal tube that should allow intra-pulmonary aerosol generation and near complete drug delivery while maintaining low air pressure and flow.

2 Experimental Setup

Aerodynamic diameter is defined as the physical diameter of a unit density sphere that settles through the air with a velocity equal to that of the particle in question. It is the most significant aerosol size parameter because it determines the particle's behavior while airborne. Particles exhibiting the same airborne behavior have the same aerodynamic diameter, regardless of their physical size, shape, density or composition.

An Aerodynamic Particle Sizer (APS 3321, TSI Incorporated) has been used, which provides high-resolution, real-time aerodynamic measurements of particles from 0.5 to 20 μm . This spectrometer uses two partially overlapping laser beams to detect coincidence. Thus, as a particle passes through these overlapping beams it generates one signal with two crests, as shown in Fig. 1. The time between the crests, which is called time-of-flight, involves measuring the acceleration of aerosol particles, with larger particles accelerating more slowly due to increased inertia. Using polystyrene latex (PSL) sphere calibration, which is stored in non-volatile memory, the spectrometer converts each time-of-flight measurement to an aerodynamic particle diameter.

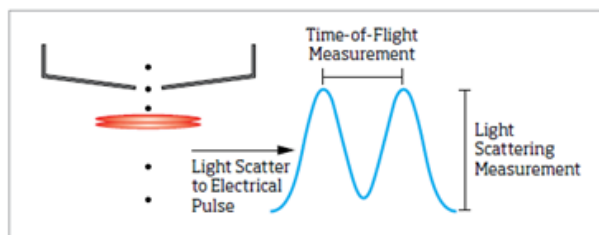


Fig.1 Double-Crested signal from particles passing through overlapping beams

An inhalation catheter (IC) (AeroProbe, Trudell Medical International), illustrated in Fig. 2, was used to produce the aerosol. In this case, sterile water (H_2O , B. Braun Melsungen, Germany; density = 0.9982 g/ml; kinematic viscosity = 1.003 cSt; surface tension = 73 dyne/cm) has been used to simulate the aerosolization at different driving pressures (4-6 bar). The compressed air is delivered through six peripheral lumens and the liquid is delivered through the central lumen. The close proximity of these lumens at the catheter tip results in efficient aerosolization of the liquid.

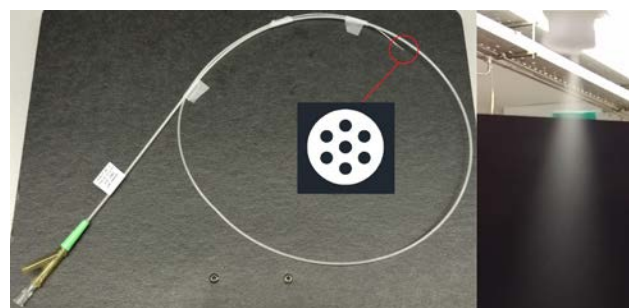


Fig. 2 Inhalation catheter IC 1.1

The IC has been connected to a pressure control system (ValveMate 7040, EFD Nordson Company), which allows to change the driving pressure

between 0-7 bar. The scheme of Fig. 3 shows the equipment and experimental setup used to study the aerosol formation. The distal end of the IC has been aligned with the nozzle of the APS in order to obtain an accurate measurement of the aerosol generated and different distances between the distal end of the IC and the nozzle has been set to check the concentration of the aerosol. Even though the usable data of the APS is up to 10.000 particles/cm³ the average recommended particle concentration is 1000 particles/cm³. The spectrometer also classifies the particles in four different events or groups in order to control the accuracy of the measurement. To obtain reliable data it is necessary to have most of the sample data classified in the second event, which measures the particles between 0.5-20 µm. The other events classify the particles smaller than 0.5 µm, particles bigger than 20 µm and the particle coincidence, which occurs when more than one particle cross the laser beams at the same time. All the data and information captured by the APS is recorded and visualized by the Aerosol Instrument Manager (TSI) software.

Six different cases were studied as can be seen in Tables 1-6 varying the driving pressure and the distance between the distal end of the catheter and the nozzle of the APS where the measurements are taken. Five samples have been recorded for each case, with a sample time of 10 seconds.

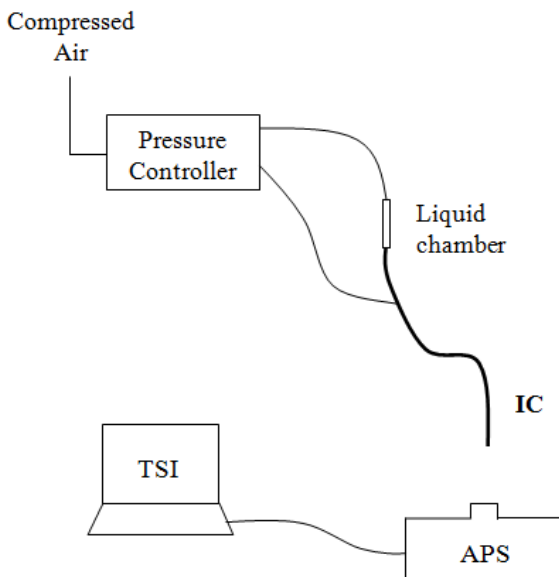


Fig. 3 Experimental set-up for the particle size characterization

The geometric standard deviation (GSD), the mass median aerodynamic diameter (MMAD) and the aerodynamic diameter (Da) have been analyzed to

study the particle size characterization. The GSD is a dimensionless number which gives an indication of the spread of sizes of particles that make up the aerosol. An aerosol is made up of particles of many different sizes (heterodisperse aerosol) with a GSD above 1.25. On the other hand, a GSD below 1.25 indicates that all the aerosol particles are of the same or very nearly the same size (monodisperse aerosol). The MMAD is defined as the value of the aerodynamic diameter (Da) such that half the mass of the aerosol is contained in small diameter particles and half in larger. The relationship between the aerodynamic particle diameter (Da) measured by the APS and the geometric particle diameter (Dg) is given by Eq. (1):

$$D_g = D_a \sqrt{\frac{\rho_0}{\rho}} \quad (1)$$

where ρ_0 is the unit density (1 g/cm³) and ρ the density of the compound to be nebulized, in this case sterile water ($\rho = 0.9982$ g/cm³)

Sample	Da (µm)	MMAD (µm)	GSD	Concentration (particles/cm ³)
1	2.64	9.59	2.16	1910
2	2.38	9.37	2.13	1740
3	2.98	9.64	2.25	1620
4	3.56	9.54	2.19	2150
5	3.39	9.65	2.24	1550
MEAN	2.99	9.56	2.19	
SD	0.49	0.11	0.05	

Table 1. Pressure: 3.5 bar; Distance IC-APS: 34.5 cm

Sample	Da (µm)	MMAD (µm)	GSD	Concentration (particles/cm ³)
6	2.69	9.83	2.26	1430
7	3.72	9.62	2.17	1860
8	4.03	9.63	2.10	1880
9	4.14	9.97	2.14	1460
10	4.16	10.1	2.12	1230
MEAN	3.75	9.83	2.16	
SD	0.62	0.21	0.06	

Table 2. Pressure: 4 bar; Distance IC-APS: 34.5 cm

Sample	Da (µm)	MMAD (µm)	GSD	Concentration (particles/cm ³)
16	4.00	10.3	2.20	1040
17	4.09	10.3	2.19	1210
18	4.08	10.1	2.15	1240
19	4.12	9.89	2.14	1060
20	4.01	10.2	2.21	1050
MEAN	4.06	10.16	2.18	
SD	0.05	0.17	0.03	

Table 3. Pressure: 4 bar; Distance IC-APS: 42 cm

Sample	Da (μm)	MMAD (μm)	GSD	Concentration (particles/cm³)
21	4.55	10.8	2.09	1020
22	4.24	10.2	2.14	879.8
23	4.33	10.6	2.16	780
24	4.51	10.5	2.06	965.3
25	4.67	10.9	2.08	917.9
MEAN	4.46	10.60	2.11	
SD	0.17	0.27	0.04	

Table 4. Pressure: 4.5 bar; Distance IC-APS: 42 cm

Sample	Da (μm)	MMAD (μm)	GSD	Concentration (particles/cm³)
27	4.54	10.4	2.09	691.3
28	4.77	11.1	2.08	671.6
29	4.76	11	2.08	671.3
30	4.83	11.1	2.04	745.6
31	4.91	11.1	1.98	1090
MEAN	4.76	10.94	2.05	
SD	0.14	0.30	0.05	

Table 5. Pressure: 5 bar; Distance IC-APS: 42 cm

Sample	Da (μm)	MMAD (μm)	GSD	Concentration (particles/cm³)
35	4.79	11.1	2.00	1310
36	4.88	10.7	1.89	1420
37	4.86	10.5	1.86	1580
38	4.89	10.1	1.84	1650
39	4.79	10.4	1.87	1530
MEAN	4.84	10.56	1.89	
SD	0.05	0.37	0.06	

Table 6. Pressure: 6 bar; Distance IC-APS: 42 cm

2.1 Total droplet mass flow rate

The aerosolization rate (AR) of sterile water has been measured according to Eq. (2). The liquid chamber was filled up and the time needed to nebulize all the liquid was controlled with a chronometer.

$$AR = \frac{(m_{cam})_t - (m_{cam})_0}{t_{pulse} \cdot \rho} \quad (2)$$

where 0 is the instant before and *t* the instant after the nebulization pulse, *m_{cam}* is the mass of the liquid chamber, *t_{pulse}* is the time of the nebulization pulse and *ρ* is the density of the sterile water. For a driving pressure of 4 bar, the 2.8 ml of sterile water that was injected to the liquid chamber through a syringe were nebulized in 85 seconds, resulting in an AR of 1.98 ml/min. The same procedure was carried out with a driving pressure of 5 bar, giving

an AR of 2.38 ml/min. The rate of liquid nebulized increased proportionally with the increase of the driving pressure.

3 Numerical model

The widespread availability of engineering workstations together with efficient solution algorithms and sophisticated pre- and post-processing methods enable the use of Computational Fluid Dynamics (CFD) techniques as a powerful tool to study and simulate the behavior of multiphase flows.

The problem has been simplified making the assumption of an axisymmetrical domain to save computational time. In this case, the six outer lumens are replaced by a ring, as shown in Fig. 4. The position of the air lumen (*b_{lcen}*) has been maintained and the width of the ring has been calculated (Eq. 3-5) in order to have the same area of the six outer lumens and consequently, the same air mass flow.

$$\text{Original total outer lumen area} = \frac{\pi d^2}{4} \cdot 6 \quad (3)$$

where *d* is the diameter of each of the six outer lumens in the distal tip, which is 66.4 μm for all of them.

$$\text{Ring Area} = 6 * \text{Outer Lumen Area} \quad (4)$$

$$\frac{\pi(b_{lcen} + x)^2}{4} - \frac{\pi(b_{lcen} - x)^2}{4} = \frac{\pi d^2}{4} \cdot 6 \quad (5)$$

where *x*, which is the width of the ring, has a value of 23.36 μm.

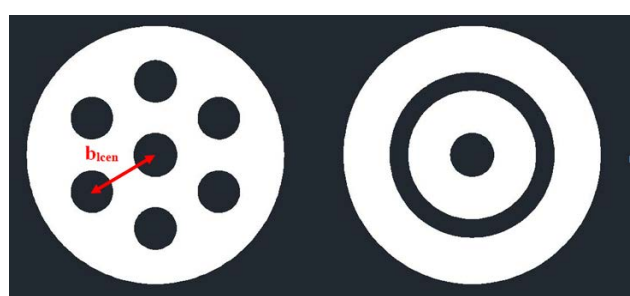


Fig.4 Original catheter distal end and the assumption used to create the axisymmetrical domain.

The computational domain consists of the last 2 mm of the catheter and the downstream region beyond the catheter tip, as illustrated in Fig. 5. An air mass flow rate of $1.1344 \cdot 10^{-5}$ kg/s, measured in a previous work with a driving pressure of 4 bar [19], was defined as the inlet boundary condition along with a

temperature of 293K and a turbulence intensity of 0.07. An atmospheric outlet boundary condition was fixed for downstream boundaries and the axisymmetrical condition was set to the central axis.

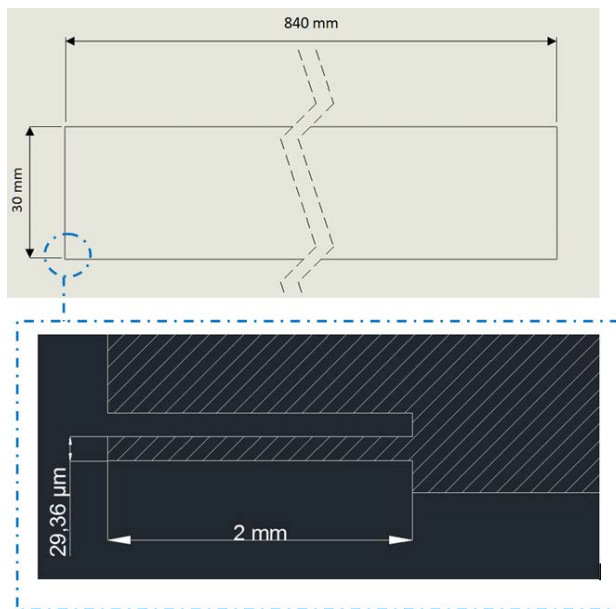


Fig. 5 Geometry of the computational domain

The discretized representation of the computational domain, which the physics solvers use to solve the Navier-Stokes equations to provide a numerical solution, consists of 887.946 cells (Fig. 6). The spatial discretization of the computational domain was generated with polygonal cells. A mesh refinement was defined near the distal tip of the IC and the axial symmetry boundary. A temporal discretization was also necessary to define the discrete phase corresponding to the sterile water droplets with a constant time-step of 1.10^{-5} s.

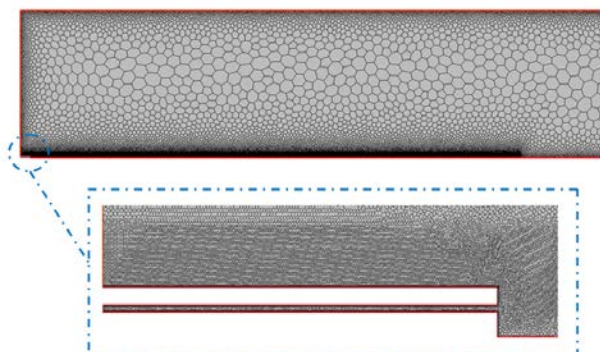


Fig. 6 Discretized representation of the computational domain

Due to the compressibility of the flow in the outlet of the catheter the pressure and velocity fields were solved with the coupled flow model, which solves the conservation equations for mass and momentum

simultaneously, providing a more robust and accurate solutions in compressible flows. The air velocity in the distal end of the catheter reaches a maximum value of 387 m/s, as can be seen in the detail of Fig 7.

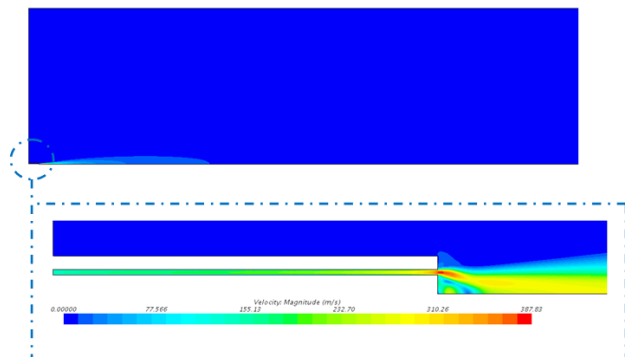


Fig. 7 Steady state air velocity

The continuity and Navier-Stokes equations are solved for the continuous phase (air) and the Newton's second law of motion is solved for the dispersed liquid droplets. Once the steady state air solution is converged the discrete phase was added by injection points defined within a line with the data of Table 7 and simulated in transient state. Fig. 8 shows the injection and the spread of the particles throughout the converged solution of the airflow. Continuous phase calculations were considered converged with a three-order-of-magnitude drop in numerical residuals. There always exist some degree interactions between the dispersed and continuous phases due to momentum exchange, heat or mass transfer, which greatly complicate two-phase flow modeling and analysis. For that reason, in this case a two-way coupling method was applied to allow the exchange of momentum between the sterile water droplets and the air flow.

Injection	D _d (μm)	m (mg/s)
1	0.375	$8.46 \cdot 10^{-4}$
2	0.562	$5.11 \cdot 10^{-4}$
3	0.841	$8.95 \cdot 10^{-3}$
4	1.26	0.0563
5	1.89	0.198
6	2.82	0.263
7	4.23	0.142
8	6.33	0.0436
9	9.18	0.0321
10	14.19	0.0108

Table 7. Data used to define the particle injections.

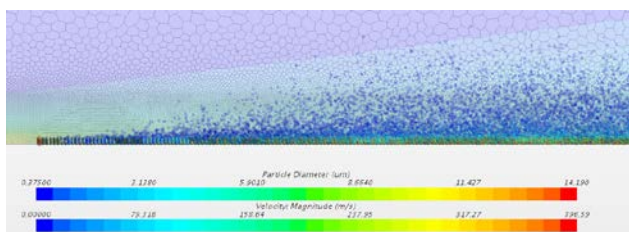


Fig. 8 Sterile water particle injections

4 Conclusion

The aerosol generated by an inhalation catheter (IC) has been studied by means of the Aerodynamic Particle Sizer (APS) along with CFD techniques. The GSD measured was between 1.89 and 2.19, resulting in heterodisperse aerosols. Note that the aerodynamic diameter (Da) was between the optimal recommended values (1-5 μm) and even though the MMAD is around 10 μm the study is focused to generate the aerosol beyond the nasopharyngeal area, avoiding the deposition of big particles.

References:

- [1] B. D. Kamath et al. Neonatal mortality from respiratory distress syndrome: Lessons for low-resource countries. *Pediatrics*, Vol.127, No.6, 2011, pp. 1139-1146.
- [2] A. Jobe and M. Ikegami. Mechanisms initiating lung injury in the preterm. *Early Human Development*, Vol.53, No.1, 1998, pp. 81-94.
- [3] A. Bhandari and V. Bhandari. Pitfalls, problems, and progress in bronchopulmonary dysplasia. *Pediatrics*, Vol.123, No.6, 2009, pp. 1562-1573.
- [4] D. G. Sweet et al. European consensus guidelines on the management of neonatal respiratory distress syndrome in preterm infants-2013 update. *Neonatology*, Vol.103, No.4, 2013, pp. 353-368.
- [5] H. Halliday et al. Multicenter randomized trial comparing high and low-dose surfactant regimens for the treatment of respiratory-distress syndrome (the curosurf-4 trial). *Arch. Dis. Child.* Vol.69, No.3, 1993, pp. 276-280.
- [6] H. Verder et al. Surfactant therapy and nasal continuous positive airway pressure for newborns with respiratory-distress syndrome. *N. Engl. J. Med.* Vol.331, No.16, 1994, pp. 1051-1055.
- [7] F. Sandri et al. Prophylactic or early selective surfactant combined with nCPAP in very preterm infants. *Pediatrics* Vol.125, No.6, 2010, pp. E1402-E1409.
- [8] P. A. Dargaville et al. Preliminary evaluation of a new technique of minimally invasive surfactant therapy. *Archives of Disease in Childhood -Fetal Neonatal Ed*, Vol.96, No.4, 2011, pp. F243-F248.
- [9] P. A. Dargaville et al. Minimally-invasive surfactant therapy in preterm infants on continuous positive airway pressure. *Archives of Disease in Childhood -Fetal Neonatal Ed*, Vol.98, No.2, 2013, pp. F122-F126.
- [10] P. A. Dargaville et al. The OPTIMIST-A trial: Evaluation of minimally-invasive surfactant therapy in preterm infants 25-28 weeks gestation. *BMC Pediatrics*, Vol.14, 2014, pp. 213.
- [11] M. Arroe et al. Inhalation of aerosolized surfactant (exosurf (R)) to neonates treated with nasal continuous positive airway pressure. *Prenatal and Neonatal Medicine*, Vol.3, No.3, 1998, pp. 346-352.
- [12] G. Jorch et al. Surfactant aerosol treatment of respiratory distress syndrome in spontaneously breathing premature infants. *Pediatric Pulmonology*, Vol.24, No.3, 1997, pp. 222-224.
- [13] E. Berggren et al. Pilot study of nebulized surfactant therapy for neonatal respiratory distress syndrome. *Acta Paediatrica*, Vol.89, No.4, 2000, pp. 460-464.
- [14] N. N. Finer et al. An open label, pilot study of aerosurf (R) combined with nCPAP to prevent RDS in preterm neonates. *Journal of Aerosol Medicine and Pulmonary Drug Delivery*, Vol.23, No.5, 2010, pp. 303-309.
- [15] J. J. Pillow and S. Minocchieri. Innovation in surfactant therapy II: Surfactant administration by aerosolization. *Neonatology*, Vol.101, No.4, 2012, pp. 337-344.
- [16] W. Burkhardt et al. Persurf, a new method to improve surfactant delivery: A study in surfactant depleted rats. *PLoS One*, Vol.7, No.10, 2012, pp. e47923.
- [17] E. Koehler et al. Lung deposition after inhalation with various nebulisers in preterm infants. *Archives of Disease in Childhood. -Fetal Neonatal Ed*, Vol.93, No.4, 2008, pp. F275-F279.
- [18] J. Dubus et al. Aerosol deposition in neonatal ventilation. *Pediatric Research*, Vol.58, No.1, 2005, pp. 10-14.
- [19] E. Goikoetxea et al. In vitro surfactant and perfluorocarbon aerosol deposition in a neonatal physical model of the upper conducting airways. *Plos One*, Vol.9, No.9, 2014, pp. e106835.

- [20] E. Goikoetxea et al. Mathematical modeling and numerical simulation of surfactant delivery within a physical model of the neonatal trachea for different aerosol characteristics. *Aerosol Science and Technology*, Vol.51, No.2, 2017, pp. 168-177.
- [21] Z. H. Syedain et al. In vitro evaluation of a device for intra-pulmonary aerosol generation and delivery. *Aerosol Science and Technology* Vol.49, No.9, 2015, pp. 746-751.